Membrane-bound Turing patterns

Herbert Levine and Wouter-Jan Rappel

Center for Theoretical Biological Physics, University of California, San Diego, 9500 Gilman Drive,
La Jolla, California 92093-0319, USA

Motivated by recent observations in biological cells, we study Turing patterns in bounded regions where the nonlinear chemical reactions occur on the boundary and where reagent transport occurs in the bulk. Within a generic model, we formulate the stability problem and discuss the conditions for the occurrence of a Turing instability. By choosing other model parameters to be unequal, we find that Turing patterns exist even in the case of equal diffusion constants. Finally, a recently introduced computation technique is utilized to follow the nascent pattern into the highly nonlinear regime.

PACS number(s): 87.10.+e, 82.40.Ck, 87.16.Ac

I. INTRODUCTION

One of the by-now familiar paradigms of pattern formation relies on the Turing instability which can occur in a variety of reaction-diffusion systems [1]. This mechanism requires an autocatalytic activation process coupled to a longer-ranged inhibition. The instability itself is characterized by having a finite wave-vector mode go unstable even as the steady-state solution remains stable to uniform perturbations. Experimental realizations of Turing pattern formation via the use of gel reactors and comparisons to models thereof have been extensively discussed [2–4].

One of the primary motivations for Turing's original suggestion was that these models might provide insight into the formation of biological patterns. Although it remains unclear how widespread the Turing paradigm really is, there have been several examples of multicellular systems which have been argued to lie in this pattern-formation class [5,6]. Our interest here, however, is to begin the investigation of Turing patterns on the single-cell scale. A specific impetus is the suggestion that reaction-diffusion patterns along the cell membrane may be implicated in the gradient-sensing machinery employed by eukaryotic cells to perform directed motion (chemotaxis). One line of evidence for this idea comes from the recent observation of spontaneous symmetry breaking in amoeboid cells exposed to *uniform* chemoattractant signals (see Fig. 1) [7]. If instead the cell is presented with a gradient, only one such spot forms and it is always at the anterior. The simplest interpretation of this data is that these cells use the external gradient to modulate an internal Turing-unstable system. This idea was originally suggested by Meinhardt [8], but he did not explicitly formulate a membrane-bound model.

Our goal here is not to propose a detailed model for this specific system; this will be presented elsewhere. Instead, we use a generic model to investigate the concept that Turing patterns can appear on membranes wherein there occur nonlinear reactions involving bulk-diffusing species. Note that this is different from previous studies of three dimensional Turing patterns which modeled uniform reaction-diffusion equations [9,10]. Models which couple intracellular diffusion to surface reactions have appeared in several biological contexts (e.g., calcium waves [11] and MIN oscillations

[12,13]), but there has not to date been a general investigation of the Turing possibility. We will demonstrate the conditions for the existence of the basic instability and will provide a computational paradigm (based on the phase-field method) for investigating the resultant nonlinear state.

II. RESULTS

A. Stability analysis

Our model is a standard two-component reaction-diffusion system where the reaction takes place on the (inner part of) the bounding surface of some bulk region. On this surface, we have

$$\dot{u}_m = -r_d u_m + r_a u + f(u_m, v_m),$$

$$\dot{v}_m = -p_d v_m + p_a v + g(u_m, v_m). \tag{1}$$

The processes whereby the bulk species u, v exchange with surface-resident ones u_m, v_m are described by the desorption coefficients r_d and p_d and adsorption coefficients r_a and p_a. A specific example of the nonlinear production functions f, g will be given later. The equations in the bulk, where no nonlinear chemistry takes place, are

$$\dot{u} = D_u \nabla^2 u - \lambda_u u,$$

$$\dot{v} = D_v \nabla^2 v - \lambda_v v$$

with as boundary condition for the normal derivatives

$$D_u \frac{\partial u}{\partial n} = r_d u_m - r_a u,$$

$$D_v \frac{\partial v}{\partial n} = p_d v_m - p_a v.$$

For simplicity, we will first work in a two dimensional circular region of radius R. The steady-state solution of the model is straightforward. In the absence of bulk decay ($\lambda_u = \lambda_v = 0$) we have constant u and v in the bulk, equal, respectively, to $r_d u_m^{(0)}/r_a$ and $p_d v_m^{(0)}/p_a$; the membrane concentra-
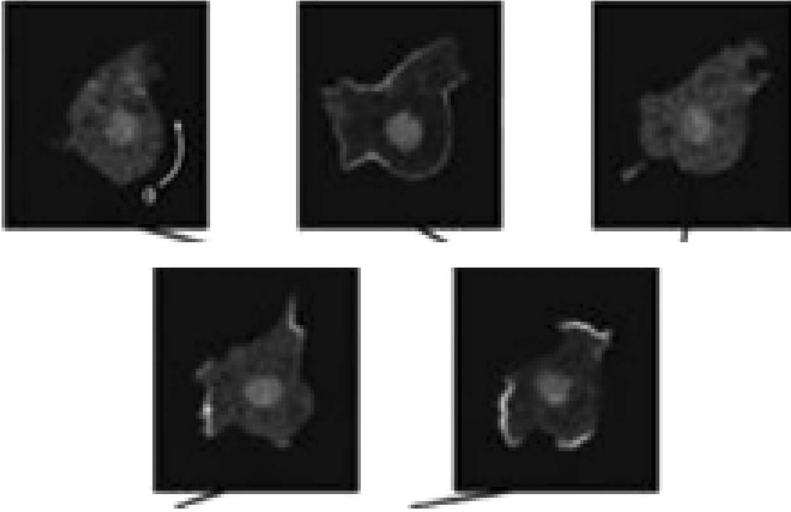
FIG. 1. Response of a Dictyostelium cell to global stimulation with 1-μM cAMP. The increased fluorescence at spots along the membrane is caused by the signal-induced attraction of Green fluorescent protein fused to a transduction protein containing a Pleckstrin-homology domain. The five pictures are (a) before stimulation; (b)–(e) 7.5, 30, 47 and 68 secs. after stimulation. From Ref. [7]

tions satisfy $f(u_m^{(0)},v_m^{(0)})=g(u_m^{(0)},v_m^{(0)})=0$. With decay, the bulk fields can be written as

$$u(r,\theta) = U^{(0)}I_0(\sqrt{\lambda_u/D_u}\,r)/I_0(\sqrt{\lambda_u/D_u}\,R),$$

$$v(r,\theta) = V^{(0)}I_0(\sqrt{\lambda_v/D_v}\,r)/I_0(\sqrt{\lambda_v/D_v}\,R). \tag{2}$$

Here, and in the remainder of the paper, I_n represents the modified Bessel function of the first kind of order n. The flux condition arising from Eq. (2) leads to

$$U^{(0)} = \frac{r_d u_m^{(0)}}{r_a + \sqrt{D_u\lambda_u}I_0'(\sqrt{\lambda_u/D_u}\,R)/I_0(\sqrt{\lambda_u/D_u}\,R)}$$

with an analogous expression for $V^{(0)}$ involving p's and the v-field diffusivity and decay constant. These are then substituted into Eq. (1), with the left hand sides set equal to zero, yielding a pair of coupled nonlinear equations for the membrane concentrations.

The stability calculation proceeds as follows. We assume that $u_m(\theta,t)=u_m^{(0)}+\delta u_m e^{in\theta}e^{\omega t}$; the corresponding perturbation in the bulk field has the same angular and time dependence and its amplitude is given by

$$\delta u(r) = A_n I_n[\sqrt{(\lambda_u+\omega)/D_u}\,r]/I_n[\sqrt{(\lambda_u+\omega)/D_u}\,R]$$

again with analogous expressions for v. Via the flux condition, we can determine that

$$A_n = \frac{r_d \delta u_m}{r_a + \sqrt{D_u k_u}I_n'(\sqrt{k_u/D_u}\,R)/I_n(\sqrt{k_u/D_u}\,R)}$$

with $k_u \equiv \lambda_u+\omega$. Doing the same for V (thereby defining a B_n coefficient) and substituting into a linearized version of Eq. (1), we obtain a 2×2 linear system,

$$\omega\delta u_m = -r_d\delta u_m + r_a A_n + f_u\delta u_m + f_v\delta v_m,$$

$$\omega\delta v_m = -p_d\delta v_m + v_a B_n + g_u\delta u_m + g_v\delta v_m. \tag{3}$$

The solvability of this system determines the growth rate ω.

To illustrate this result, we focus on the specific case of $f(u_m,v_m)=a(u_m^2 v_m-u_m)$ and $g(u_m,v_m)=1-u_m^2 v_m$ introduced by Gierer and Meinhardt [14]. In general, the pair of coupled

nonlinear equations for the membrane concentrations can be solved numerically. For our specific case, however, we can solve these equations analytically. For the case without bulk degradation, $\lambda_u=\lambda_v=0$, the solution is simply $u_m^{(0)}=v_m^{(0)}=1$, and thus $U^{(0)}=r_d/r_a$ and $V^{(0)}=p_d/p_a$. With degradation, we find three solutions for $u_m^{(0)}$: $u_m^{(0)}=0$ and

$$u_m^{(0),\pm} = \frac{-a \pm \sqrt{a^2-4(M_u-a)(M_v a-M_u M_v)}}{2(M_u-a)},$$

where M_u is given by

$$M_u = \frac{-r_d\sqrt{\lambda_u D_u}I_0'(\sqrt{\lambda_u/D_u}\,R)/I_0(\sqrt{\lambda_u/D_u}\,R)}{r_a + \sqrt{\lambda_u D_u}I_0'(\sqrt{\lambda_u/D_u}\,R)/I_0(\sqrt{\lambda_u/D_u}\,R)}.$$

M_v is given by a similar expression and $v_m^{(0)}$ can be found via $v_m^{(0)}=1/[(u_m^{(0)})^2-M_v]$. We will focus here on relevant nonzero solutions for $u_m^{(0)}$, which turns out to be the negative root solution.

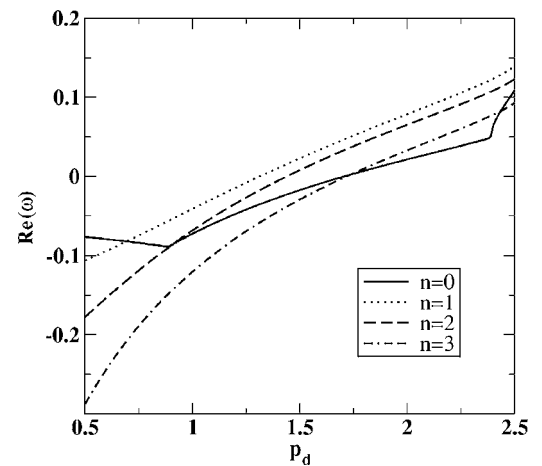In Fig. 2, we plot the the largest growth rate for the modes

FIG. 2. The largest growth rate ω as a function of p_d for the first four modes. Parameter values, in arbitrary dimensionless units, are $r_a=r_d=p_a=D_u=1$, $a=0.4$, $D_v=10$, $\lambda_u=\lambda_v=0.02$, and $R=8$.
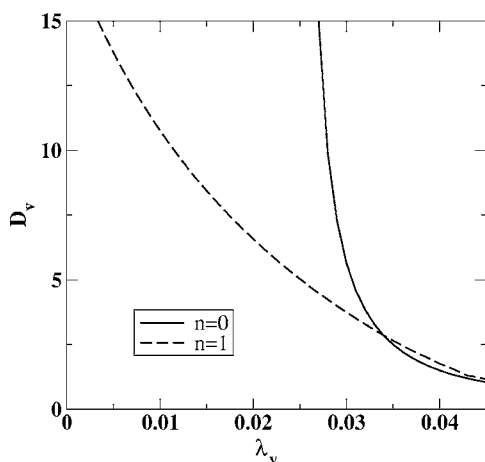
FIG. 3. Phase diagram showing the stability boundary of the $n=0$ (solid line) and the $n=1$ mode (dashed line). Parameter values are as in Fig. 2 but with $p_d=1.5$. The modes are unstable to the right of the curve.

$n=0$ through $n=3$ for a sweep over the parameter p_d with everything else being held fixed. The fact that there is a range for which the $n=0$ mode has negative growth rate whereas some higher n have positive ones indicate the existence of a Turing instability. Figure 3 shows a two parameter phase diagram where we vary the diffusion constant D_v (keeping D_u fixed at 1) and the decay rate λ_v (keeping λ_u fixed at 0.02). As expected, long-range variation of the v field as enabled by large D_v and small λ_v drive the $n=1$ instability. We note in passing that it is possible to tune the system to a co-dimension two point for which the Turing instability occurs simultaneously with an $n=0$ Hopf bifurcation. We also note that it is straightforward to include diffusion along the membrane. This inclusion leads in Eq. (3) to the replacements $r_d \rightarrow r_d + n^2 D_{u_m}$ and $p_d \rightarrow p_d + n^2 D_{v_m}$, where D_{u_m} and D_{v_m} are the diffusion constants of u_m and v_m, respectively. Typical membrane diffusion constants are much smaller than bulk diffusion constants. Thus for biological realistic values of D_{u_m} and D_{v_m}, membrane diffusion will have an appreciable stabilizing effect only for large n modes. Finally, in Fig. 2 both the diffusion and the desorption coefficients are unequal. However, we have checked that a Turing instability also exists for equal desorption coefficients and unequal diffusion coefficients.

B. Simulations using the phase-field method

Let us now extend our calculations to three dimensions. The stability calculation proceeds as before, with the only difference being that the bulk solutions are now given by modified spherical Bessel functions. To check the validity of our stability results and to study the restabilized nonlinear state, we performed numerical simulations of the equations on a sphere of radius R. Unfortunately, traditional finite difference methods are not able to handle curved boundaries. One solution would be to reformulate the problem using a finite elements approach. Here, however, we have chosen to utilize the phase-field method to numerically solve the original system [15,16].

This method has traditionally been used to solve a variety of free boundary problems, including dendritic solidification [17], viscous fingering [18], crack propagation [19,20], and the tumbling of vesicles [21], but can also be applied to tackle diffusional problems in stationary but complicated geometries [22,23]. It can handle the boundary conditions correctly and offers an accurate, computationally inexpensive method that can be implemented with ease. Its main advantage is that it avoids the need for explicit interface tracking by introducing an auxiliary field that locates the interface and whose dynamics is coupled to the other physical fields through an appropriate set of partial differential equations. In comparison to the more traditional boundary integral methods, the method is much simpler to implement numerically.

In our case, the equation of motion for the field u becomes

$$\frac{\partial u}{\partial t} = D_u \frac{\vec{\nabla} \cdot [\phi \vec{\nabla} u]}{\phi} - \lambda_u u + (r_d u_m - r_a u)\frac{(\vec{\nabla}\phi)^2}{K\phi}, \qquad (4)$$

where K is a normalization constant which depends on the area A of the membrane: $K = \int d\vec{x}(\vec{\nabla}\phi)^2/A$. The time evolution for v is given by a similar equation. The phase field ϕ is chosen to have the explicit form

$$\phi(r) = \frac{1}{2} + \frac{1}{2}\tanh[(r_0 - r)/\xi]. \qquad (5)$$

Thus the phase field has the value +1 inside the cell, 0 outside the cell and varies between these two values across a diffusive boundary layer of thickness ξ. One can show that in the limit of $\xi \rightarrow 0$ the appropriate boundary conditions are recovered [22]. Equation (4) is solved on a regular cubic grid in a computational box that can easily fit the geometrical object. The equations for the bulk diffusion were solved using an alternating-direction method while the equations for the membrane variables u_m and v_m were solved on all grid points where $(\vec{\nabla}\phi)^2$ exceeds a certain threshold, namely 10^{-4}.

In Figs. 4(A)–4(D), we show snapshots of the time evolutions of the u field on the membrane. As initial conditions we started with uniform values for the fields plus a small amount of noise in the u field. In Fig. 4(E) we plot the value of u at one point of the membrane as a function of time. The snapshots in Figs. 4(A)–4(D) correspond with the points labeled A–D. As we can see, after a transient, the uniform solution destabilizes and a Turing pattern emerges on the membrane. We have verified that a similar pattern arises when using a smaller gridspacing, indicating the absence of any grid induced effects.

C. Turing patterns for equal diffusion constants

The unusual ingredient of bulk diffusion, coupled to nonlinear membrane dynamics, leads to phenomena not seen in ordinary Turing systems. In ordinary Turing systems, it can be shown that a Turing instability cannot occur when all diffusion constants are exactly equal [[24], and references therein]. Here, however, as in nonuniform multicellular systems [25], it becomes possible for a Turing pattern to develop even in the case $D_u = D_v$. The necessary difference in activator and inhibitor transport can then be provided by
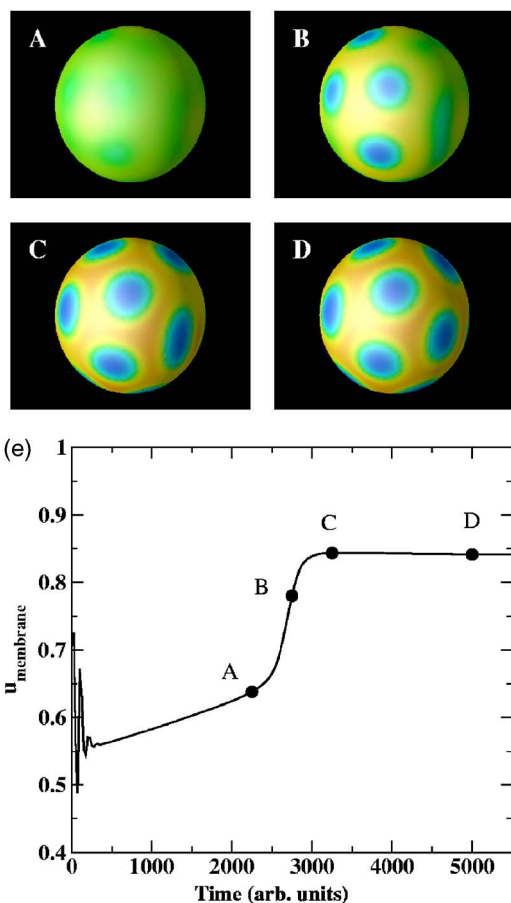
FIG. 5. The system can exhibit Turing patterns even in the case of equal diffusion constants. Shown here is u_m along the membrane of a circular region, parametrized by the angle θ. Parameter values are $D_u=D_v=2$, $r_a=p_a=1$, $r_d=0.1$, $p_d=0.3$, $a=0.05$, $\lambda_u=1$, $\lambda_v=0.3$, and $R=2$. The simulation utilized the phase field with a width of $\xi=0.2$ and a computational box containing a rectangular grid with dimensions 120×120. For plotting purposes, the membrane is defined as the points of the rectangular grid that are closest to the perimeter of the disk. Consequently, the plotted field exhibits some variation which has been reduced by a smoothing procedure.

we have not performed a completely systematic exploration of parameter space. In passing, we note that a traveling-wave mode is believed to be responsible for the intracellular oscillations observed in E. coli [13].

FIG. 4. (Color online) A–D snapshots of the variable u at the membrane of the sphere of radius $R=50$. The parameter values are $a=0.7$, $p_d=1.25$, $\lambda_u=\lambda_v=0.01$, $D_u=1$, and $D_v=10$. The width of the phase field is taken as $\xi=5$ and the computational box has dimensions $100\times100\times100$. (E) The value of u at an arbitrarily chosen point of the membrane as a function of time with the points A–D corresponding to the snapshots.

choosing other parameters (desorption, adsorption or decay rates) to be unequal. An example of this case is shown in Fig. 5, where we plot the final, steady-state membrane concentration u_m along the membrane. The example is in a two dimensional disk of radius R but we have verified that a similar instability exists in three dimensions. As initial conditions, we used uniform values of the fields plus a small perturbation favoring the $n=1$ mode. In the case of equal diffusion constants, we have also found time-varying inhomogeneous solutions, corresponding to traveling-wave instabilities with complex eigenvalues. In fact, this alternative instability seems to be the dominant one for equal diffusion, although
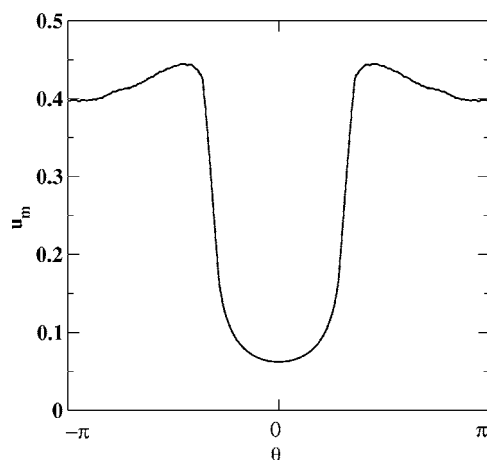
III. CONCLUSION

In summary, we have studied the generic properties of a new class of Turing instability, one arising from restricting the reactions to occur on a bounding membrane. This type of dynamics is generic in signal transduction systems within single cells. Interestingly, we found that in this system the condition of a faster diffusion inhibitor no longer is necessary and that Turing patterns exists even for equal diffusion constants. Our results form the underpinning for more detailed modeling of Turing patterns in specific biological contexts.

ACKNOWLEDGMENTS

[1] A. Turing, Philos. Trans. R. Soc. London, Ser. B **237**, 37 (1952).

[2] V. Castets, E. Dulos, J. Boissonade, and P. De Kepper, Phys. Rev. Lett. **64**, 2953 (1990).

[3] Q. Ouyang and H. L. Swinney, Nature (London) **352**, 610 (1991).

[4] I. Lengyel and I. R. Epstein, Science **251**, 650 (1991).

[5] J. D. Murray, *Mathematical Biology* (Springer-Verlag, Berlin, 1993).

[6] H. Meinhardt, *The Algorithmic Beauty of Sea Shells* (Springer-

Verlag, Berlin, 2003).

[7] M. Postma, J. Roelofs, J. Goedhart, T. W. Gadella, A. J. Visser, and P. J. van Haastert, Mol. Biol. Cell **14**, 5019 (2003).

[8] H. Meinhardt, J. Cell. Sci. **112**, 2867 (1999).

[9] C. Varea, J. L. Aragón, and R. A. Barrio, Phys. Rev. E **60**, 4588 (1999).

[10] T. Leppänen, M. Karttunen, R. A. Barrio, and K. Kaski, Phys. Rev. E **70**, 066202 (2004).

[11] B. Pando, J. E. Pearson, and S. P. Dawson, Phys. Rev. Lett. **91**, 258101 (2003).

[12] M. Howard, A. D. Rutenberg, and S. de Vet, Phys. Rev. Lett. **87**, 278102 (2001).

[13] K. C. Huang, Y. Meir, and N. S. Wingreen, Proc. Natl. Acad. Sci. U.S.A. **100**, 12724 (2003).

[14] A. Gierer and H. Meinhardt, Kybernetik **12**, 30 (1972).

[15] J. B. Collins and H. Levine, Phys. Rev. B **31**, R6119 (1985).

[16] J. S. Langer, *Directions in condensed matter physics. Memorial volume in honor of Sheng-keng Ma* (World Scientific, Singapore, 1986), pp. 165–86.

[17] A. Karma and W. -J. Rappel, Phys. Rev. E **57**, 4323 (1998).

[18] R. Folch, J. Casademunt, A. Hernandez-Machado, and L. Ramirez-Piscina, Phys. Rev. E **60**, 1724 (1999).

[19] I. S. Aranson, V. A. Kalatsky, and V. M. Vinokur, Phys. Rev. Lett. **85**, 118 (2000).

[20] A. Karma, D. A. Kessler, and H. Levine, Phys. Rev. Lett. **87**, 045501 (2001).

[21] T. Biben and C. Misbah, Phys. Rev. E **67**, 031908 (2003).

[22] J. Kockelkoren, H. Levine, and W. -J. Rappel, Phys. Rev. E **68**, 037702 (2003).

[23] F. H. Fenton, E. M. Cherry, A. Karma, and W. -J. Rappel, Chaos **15**, 13502 (2005).

[24] J. E. Pearson and W. Horsthemke, J. Chem. Phys. **90**, 1588 (1989).

[25] E. M. Rauch and M. M. Millonas, J. Theor. Biol. **226**, 401 (2004).